Lead (Pb) profiles in red coral skeletons as high resolution records of pollution in the Mediterranean Sea

Angèle Ricolleau, Nicole Floquet, Jean-Luc Devidal, Robert Bodnar, Jonathan Perrin, Joaquim Garrabou, Jean-Georges Harmelin, Federica Costantini, Joana Boavida, Daniel Vielzeuf

Lead profiles in red coral skeletons as high resolution records of pollution in the Mediterranean Sea

Angèle Ricolleau[1], Nicole Floquet[1], Jean-Luc Devidal[2], Robert J. Bodnar[3], Jonathan Perrin[4], Joaquim Garrabou[5], Jean-Georges Harmelin[6], Federica Costantini[7], Joana R. Boavida[8] and Daniel Vielzeuf[1*]

[1]Aix Marseille Université, CNRS, Centre Interdisciplinaire de NanoScience de Marseille, UMR 7325, 13288 Marseille, France
[2] Laboratoire Magmas et Volcans, Université Blaise Pascal – CNRS - IRD, OPGC, 6 Avenue Blaise Pascal, campus universitaire des Cézeaux, 63178 Aubière, France
[3] Department of Geosciences, Virginia Tech, 4044 Derring Hall, 926 West Campus Drive, Blacksburg, VA 24061, USA
[4] Synchrotron SOLEIL, L'Orme des Merisiers, Saint-Aubin, BP48, 91192 Gif-sur-Yvette, France
[5] Institut de Ciencies del Mar – CSIC, Passeig Maritim de la Barceloneta 37-49, 08003 Barcelona, Spain
[6] Aix Marseille Université, OSU Pytheas, Mediterranean Institute of Oceanography (MIO), Station Marine d'Endoume, 13007 Marseille, France
[7] Università di Bologna, Dipartimento di Scienze Biologiche, Geologiche ed Ambientali BiGeA, Via S. Alberto 163, 48123 Ravenna, Italy
[8] Aix Marseille Université, CNRS/INSU, Université de Toulon, Mediterranean Institute of Oceanography (MIO) UM 110, 13288 Marseille, France

* *Corresponding author:* D. Vielzeuf, vielzeuf@cinam.univ-mrs.fr

Abstract

Lead concentrations in long-lived *Corallium* species of known age, from the Mediterranean Sea, Atlantic and Pacific Oceans, were determined by laser ablation, inductively coupled plasma mass spectrometer (LA-ICPMS). Lead concentrations in a 2000-year-old sub-fossil Mediterranean *C. rubrum* are ca 0.09 ± 0.03 µg/g. For the period 1894-1955, lead concentrations in *C. rubrum* skeletons from the Mediterranean are stable within the range 0.2-0.4 µg/g; concentrations increase to about 1-1.2 µg/g during the period 1960-1978, then decrease progressively to stabilize and reach values in the range 0.2-0.4 µg/g in present-day corals. These variations can be related to the lead gasoline pollution event that (1) started in the early 1950s with the increase of the numbers of cars in the world, and (2) was mitigated by the implementation of new regulations starting in 1975, leading to a return to pre-1950 levels in 2000. In the Pacific, lead concentrations in *C. japonicum* and *C. konojoi* are lower than in the Mediterranean *C. rubrum*, with values close to 0.17 ± 0.03 µg/g. The lowest lead concentrations in present-day samples (0.11 µg/g) are found in *C. johnsoni* and *C. niobe* from the Azores islands in the Atlantic, and in a Mediterranean *C. rubrum* from Montecristo Island, one of the least accessible and most protected areas in the Mediterranean Sea. Using lead concentrations in *C. rubrum* and in the Mediterranean seawaters, a partition coefficient $Kd = [Pb/Ca]_{calcite} / [Pb/Ca]_{seawater}$ of 13 +/-3 is estimated; it allows calculating past and present lead contents in seawater in which corals grew. Application to *Corallium* species indicates that values endangering human health or threatening the preservation of aquatic ecosystem on long terms were nearly reached or exceeded in Mediterranean seawaters at the maximum of the lead gasoline pollution event in the 1980s. Measurements in *C. rubrum* from different places in the Mediterranean indicate that present-day seawater concentrations vary between

40 and 200 pmol/kg. As expected, the lowest concentrations come from protected areas insulated from human activities, while the highest come from places close to lead mining or processing sites.

Keywords

Lead, *Corallium*, Calcite, Seawater, Partition coefficient, Diagenesis, Sciacca

Highlights

- Lead contents in *Corallium* skeletons record the lead gasoline pollution event (1950-2000)
- Lead contents are lower in Atlantic and Pacific corals than in the Mediterranean
- Levels endangering the preservation of aquatic ecosystems were reached in the 1980s
- Lead contents in present-day Mediterranean corals returned to pre-1950 levels

1. Introduction

Biominerals have been used routinely as proxies of environmental conditions through compositions in major, minor, trace elements and isotopes [e.g. Chave (1954); Epstein and Lowenstam (1953)]. Among biominerals, biogenic calcium carbonates are able to incorporate different elements in significant amounts. In the case of *Corallium* species, these include magnesium, strontium, sodium, sulfur, lithium, barium, lead and uranium [see Vielzeuf et al. (2018); Vielzeuf et al. (2013) for summaries]. However the ability to incorporate an element is not a guarantee of a faithful environmental proxy as concentration variations can also be due to biological or physico-chemical effects, or combinations of factors. Thus, the potential of each element as a proxy in a given species has to be tested. The precious red coral *Corallium rubrum* (*Cnidaria, Anthozoa, Octocorallia*) is an emblematic species of the western Mediterranean but is also present in the Atlantic Ocean along the southern coast of Portugal, and along the coast of Morocco (Zibrowius et al., 1984). The red coral grows within a large range of depths from near-surface down to ~1000 m (Costantini et al., 2010; Knittweis et al., 2016). This colonial organism has a ramified erect growth-form and a skeleton made of high magnesian calcite (Lacaze-Duthiers, 1864). Its skeleton has a slow radial growth of

about 100 to 200 µm per year (Marschal et al., 2004) and can live several decades (Garrabou and Harmelin, 2002). In a companion paper, it has been determined that growth kinetics plays a role in the incorporation of Mg, Na, Sr, Li, S and U in the skeletons of *Corallium* species (Vielzeuf et al., 2018). Conversely, it was shown that growth kinetics does not influence the incorporation of Ba and Pb. Concerning lead, large variations of concentrations in corals were observed (Vielzeuf et al., 2018). These data raised the question of the origin and significance of the variations of lead in *Corallium* skeletons. It is a well-known fact that human activities resulted in massive release of lead into the earth surface (Boutron et al., 2004; Patterson, 1965; Wu and Boyle, 1997). Paleo-environmental and archaeological records suggest that lead pollution started as early as the Chalcolithic (~5000 cal. Yr. BP) (Martinez-Cortizas et al., 1997; Martinez Cortizas et al., 2016; Settle and Patterson, 1980). Most importantly, the use of lead additives in gasoline initiated in 1923 created a public health problem worldwide (Patterson, 1965). In this study, we determine the lead concentrations in the skeletons of *Corallium* species by LA-ICPMS and discuss the incorporation of lead in biogenic high magnesian calcites. The question whether the lead content in red coral skeletons is a potential proxy of the concentration of lead in the Mediterranean Sea is also addressed. Concentration profiles at annual-scale resolution are obtained in *C. rubrum* skeletons of different ages and provenances. The discussion is extended toward *Corallium* species from the Atlantic (*C. rubrum, C. niobe* and *C. johnsoni*) and the Pacific (*C. japonicum* and *C. konojoi*). Finally, the results are compared to other lead records in the Mediterranean basin, in the Atlantic and Pacific Oceans, and in polar ice cores.

2. Material and methods

2.1. Samples

2.1.1 *C. rubrum*

Present day C. rubrum - Analytical profiles were mainly performed on five modern colonies of *C. rubrum* with known place and date of sampling. The colonies were collected (i) at Riou Island (Marseille, France) in 2002, (ii) in the Calanques area near Cassis (France), in a 15 m depth marine cave (the Tremies cave) in 2010, (iii) near the Medes Islands (L'Estartit, Spain) in 2002 and 2014, and (iv) near Cap de Creus (Spain) in 1962. Figure 1 shows a map with the original locations of the colonies. Samples were collected at depths varying between 15 m and 73 m, i.e. in the range of surface waters.

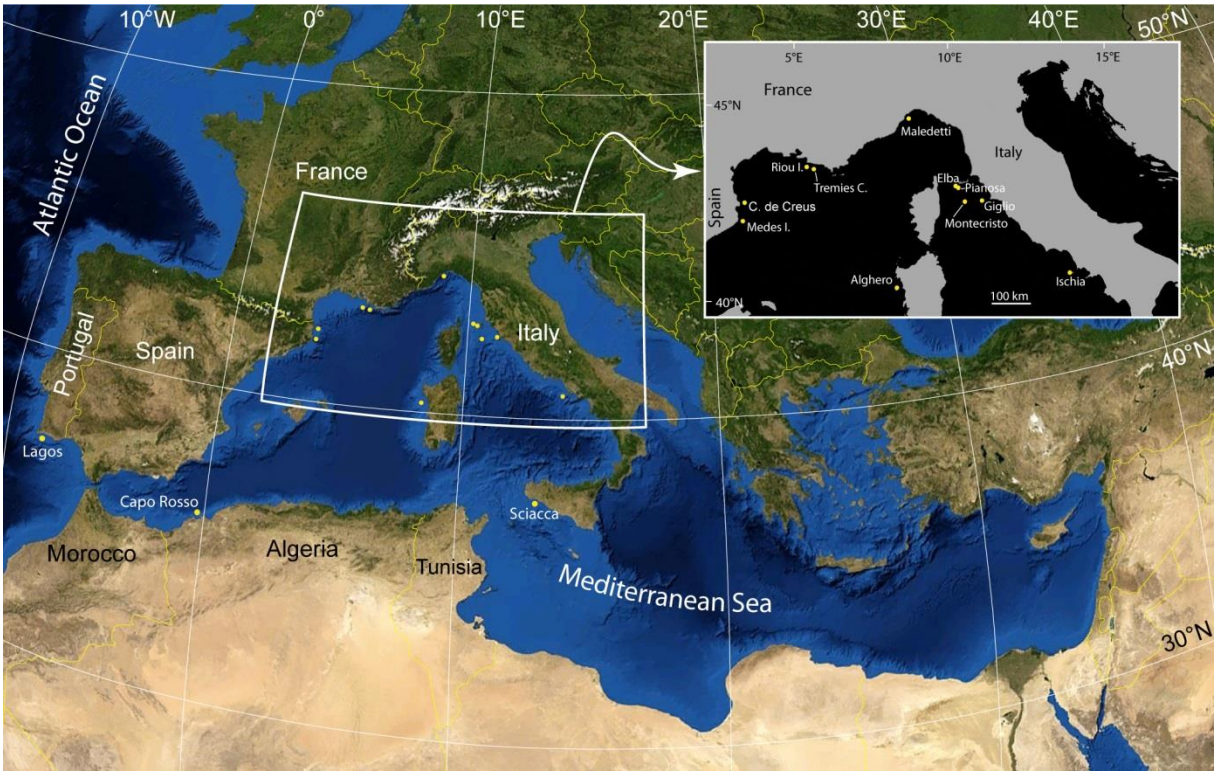

***Figure 1**: Map of the north-western Mediterranean Sea with locations of the studied samples.*

Additional LA-ICPMS analyses (not necessarily along analytical traverses) were carried out on recent colonies from Algeria and Italy (including Montecristo island), to enlarge our vision of lead contents in the Mediterranean (Table 1 – supplementary materials).

Sub-fossil C. rubrum samples – A sub-fossil sample of *C. rubrum* skeleton buried in the sediments of the Tremies Cave was collected in 2007. Its absolute age was determined as 1950 ±30 years BP by ^{14}C dating in the Poznań Radiocarbon Laboratory.

Quite surprisingly, huge amounts of red coral collected in Italy in the last 150 years came from the sub-fossil coral reservoir of the Sciacca Banks (Sicily Channel) where 18,000 tons were collected in 34 years (Cattaneo-Vietti et al., 2016; Rajola, 2012). Large uncertainties still exist on the age of these sub-fossil colonies, but four samples were carbon dated at University of Salento (Italy) and provided ages between 2000 and 10,000 years BP (Rajola, 2012). In this study, we present LA-ICPMS data on a Sciacca sub-fossil sample whose age has not been determined, but is assumed to be in the range 2,000-10,000 years BP.

Independently from the analyses carried out in France, other present-day Mediterranean *C. rubrum* samples from Spain, Italy, North Africa, and sub-fossil Sciacca corals (Sicily, Italy) were analyzed at Virginia Tech. (USA) and these data will be presented and discussed here. Two samples of the Sciacca corals were dated by radiocarbon and gave ages of 2400-2100 years BP and 4400-4050 years BP (Rajola, 2012).

C. rubrum from the Atlantic - In Portugal, coral fisheries were abandoned about 300 years ago (Zibrowius et al., 1984). Recently, *C. rubrum* colonies were re-discovered in Southern Portugal (Boavida et al., 2016). Two rare samples from Sagres (Lagos Portimão) collected at 90m depth (Boavida et al., 2016) were also studied by LA-ICPMS.

2.1.2 - Other *Coralliidae*

Skeletons of *Corallium niobe* and *C. johnsoni* from the Atlantic (Azores Islands) have been collected in 2005 and 2011, respectively, and two specimens of *Corallium* species from the Pacific (C. *japonicum* and *C. konojoi*) have been harvested along the Japan coast in 2013 and 2015, respectively.

Geographic locations, depths and sampling dates of all samples are given as supplementary materials in Table 1, and in Vielzeuf et al 2018 (supplementary materials, Table 1).

2.2 Preparation of the samples, growth rings identification, and age determination

Contrary to banded scleractinian corals made of aragonite, *Corallium* species have dense skeletons without marked porosity. For this reason and because of the selected analytical technique (LA-ICPMS), no cleaning preparative sequence of the samples was necessary, as is the case for scleractinian corals [e.g. Shen and Boyle (1988)]. For each colony, one or two branches were cut transversally, mounted in epoxy, and polished with diamond paste down to 0.25 µm.

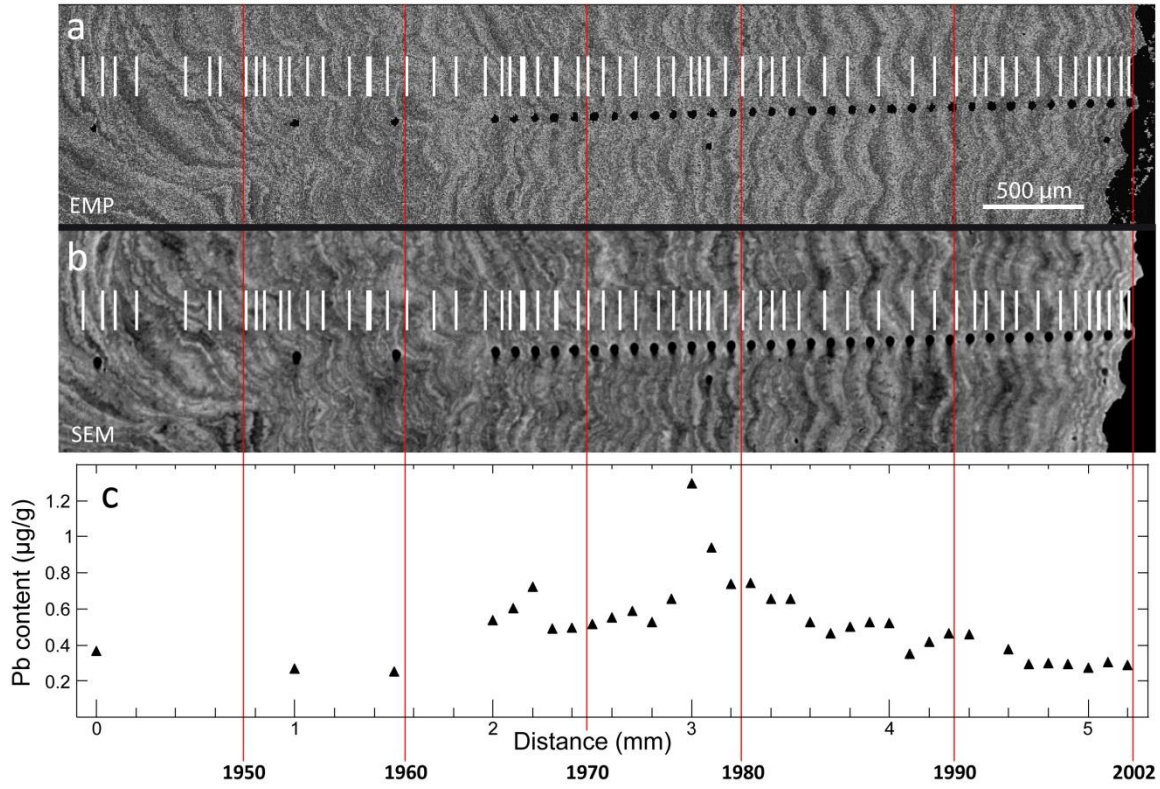

Figure 2*: EMP Mg map and SEM images. a) Electron microprobe map of magnesium and LA-ICPMS profile in a sample collected near the Medes Islands in 2002. The contrast has been inverted for a better comparison with the SEM image (bright to dark – low to high Mg contents). The white vertical lines mark each annual growth ring. The black dots (40 µm in diameter) are the locations of the LA-ICPMS analyses. b) Mosaic of SEM images of the same area. c) Pb concentrations obtained in the LA-ICPMS profile (see figure 4 for other profiles).*

It has long been known that *C. rubrum* skeletons display growth rings (Lacaze-Duthiers, 1864). By surveying colonies over long periods of time, Garrabou and Harmelin (2002) determined the axial (height) and radial (diameter) growth rates of *C. rubrum* colonies

as 1.8 mm and 0.25 mm year^{-1}, respectively. Concomitantly, Marschal et al. (2004) developed a method to identify growth rings by staining the organic matrix. Annual growth rings are about 100 to 200 µm thick (Marschal et al., 2004). These authors demonstrated the annual periodicity of the growth rings by *in situ* calcein labeling of some colonies. Then, it was demonstrated that growth rings are also marked by variations of magnesium (Vielzeuf et al., 2008; Vielzeuf et al., 2013). These variations can be detected by electron microprobe (EMP) mapping, but also by scanning electron microscopy (SEM) using backscattered electron (BSE) imaging. Mg-rich rings appear darker than Ca-rich rings in SEM BSE images because Mg has a lower atomic number (Z) than Ca. The exact correlation between Mg-rich rings observed by electron probe and dark rings in BSE images can be observed in Figure 2a and 2b. Note that in EMP maps low concentrations normally appear in black. However, for a better comparison of EMP and SEM images, the contrast of the EMP image was inverted in Fig. 2 (dark layers indicate high concentrations of Mg). In the present study, SEM was the main method used to image the growth rings because of its non-destructive character (contrary to OM staining) and faster and easier implementation than EMP Mg mapping. As colonies with known sampling date were selected, the absolute age of each growth ring could be determined. Figures 2a to 2c show an example of correlation between growth ring, spatial location, age and lead content in a sample collected in 2002 (Medes sample). The error on the determination of the number of annual rings is estimated to be ± 10% relative.

2.3 Analytical Methods

2.3.1 Electron microprobe and SEM mapping

Electron microprobe chemical images of magnesium were obtained on thick polished samples embedded in epoxy, on a SX100 CAMECA electron microprobe [Laboratoire Magmas et Volcans (LMV), Clermont-Ferrand, France]. For image acquisition, the beam current, beam diameter, counting times, and step interval varied in the range 10–50 nA, 1–2 mm, 30–50 ms

per pixel, 1–5 mm, respectively, with an acceleration voltage of 15 kV. All samples were coated with an ~20 nm thick carbon layer.

All samples (including those studied by EMP) were examined with a field-emission scanning electron microscope (FESEM) Raith Pioneer at CINaM (Marseille) in order to image both growths rings and the ablation spots, and to correlate age and lead concentrations. Images were obtained in BSE mode, with 20 kV accelerating voltage, 9.5 nA probe current, and 6 mm working distance. To obtain clear images of entire analytical profiles, images at a high spatial resolution were treated by Fourier transforms to enhance contrast (Perrin, 2014), and assembled into large mosaics (see Figure 2b and Figure 5a).

2.3.2 Laser ablation ICP-MS

Most laser ablation inductively coupled plasma mass spectrometry (LA-ICPMS) analyses were conducted at Laboratoire Magmas et Volcans in Clermont-Ferrand (France). Trace element concentrations in calcite skeletons were obtained using an Agilent 7500-cs ICPMS coupled to an Excimer Resonetics M-50 laser. The laser was operated at 193 nm wavelength with 6-8 mJ energy, and 2-3 Hz pulse frequency. Spot size was 40 µm, with a spacing interval of 100 µm in most analytical traverses. Ablation duration lasted about 100 s (blank count rates were measured for 30 s prior to 70 s of ablation) in pure He atmosphere. The analyte was carried to the ICP torch by a gas mixture wherein N_2 + Ar were added to He. NIST 610 glass standard was used for calibration (Gagnon et al., 2008). NIST 610 and BCR glasses were analyzed every 15-20 spots as checks for precision. Duplicate analyses were obtained for some coral samples to check for drift and to confirm the reproducibility of the results from one session to another. Internal instrumental (1σ) errors and detection limits for lead are most frequently both within the range 0.01-0.02 µg/g, and always below 0.04 µg/g. Data were processed with the GLITTER software (Van Achterbergh et al., 2001).

206 At Virginia Tech, minor and trace element abundances of coral samples were
207 determined by LA-ICPMS using an Agilent 7500ce quadrupole ICP-MS and a Lambda
208 Physik GeoLas 193 nm ArF excimer laser ablation system. The laser is coupled to an
209 Olympus petrographic microscope equipped with a 25× UV and visible Schwarzschild
210 objective (NA = 0.4) for analysis, plus 5× and 10× objectives for sample viewing. Four to six
211 spots were analyzed in each of 7 samples using a 60 µm spot size. He carrier gas flowed
212 through an ablation cell with a volume of ~1 cm^3 at a flow rate of ~ 60 mL/min. Dwell times
213 were 10 ms for all elements and the oxide production rate was less than 1%. [Additional
214 information concerning the system is available at: http://www.geochem.geos.vt.edu/fluids/].
215 NIST 610 standard reference material (SRM) glass was analyzed two times before and after
216 each analytical session and was used as the external standard for data reduction and for drift
217 correction (Mutchler et al., 2008). Analyses of the NIST glass were accomplished using a
218 discharge voltage of the laser of 27 kV and a pulse rate of 15 Hz. The energy density at the
219 sample is a function of the aperture and attenuator settings which, for the analytical conditions
220 used here, results in an energy density on the sample of about 10±3 J/cm^2. Isotopes analyzed
221 included ^{7}Li, ^{11}B, ^{23}Na, ^{25}Mg, ^{27}Al, ^{28}Si, ^{39}K, ^{40}Ca, ^{49}Ti, ^{55}Mn, ^{56}Fe, ^{63}Cu, ^{66}Zn, ^{75}As,^{88}Sr, ^{89}Y,
222 ^{90}Zr, ^{93}Nb, ^{138}Ba, ^{139}La, ^{140}Ce, ^{143}Nd, ^{147}Sm, ^{153}Eu, ^{157}Gd, ^{163}Dy, ^{166}Er, ^{172}Yb, ^{208}Pb, ^{232}Th and
223 ^{238}U. Calcium was used as an internal standard assuming a stoichiometric concentration of
224 calcium in the calcium carbonate. For each LA-ICPMS analysis, background signal was
225 collected for approximately 30-40 seconds before the laser shutter was opened to begin to
226 ablate the sample. The ablation was stopped after a few 10s of seconds and the signal was
227 collected until intensities returned to background levels. The initial few seconds of data from
228 each analysis was not included in data reduction to avoid possible errors from contamination
229 on the sample surface from airborne particles or previously ablated material deposited onto

the surface. Only the relatively stable, flat-topped portion of the ablation spectrum was used to calculate element abundances.

3. Results

3.1 Lead contents and profiles in recent C. rubrum skeletons from the Mediterranean

The sample collected in 1962 near Cap de Creus (Spain) provides lead contents down to the late nineteenth century period (~1894 AD). A first profile was obtained in the basal part of the colony, providing a larger time span than a second profile collected in the upper part of the colony. Figure 3 shows the lead content as a function of time along two profiles.

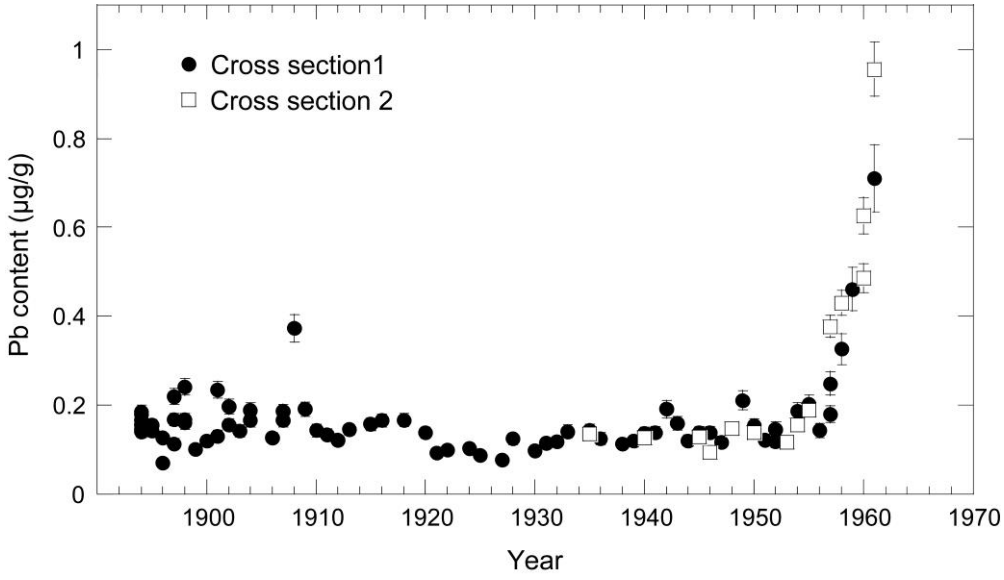

***Figure 3**: Two Pb profiles obtained in a C. rubrum colony from Cap de Creus collected in 1962.*

A good correlation is observed between the two profiles that display a flat signal with low Pb levels between 1900 and 1955 followed by a sharp increase in the Pb content starting in 1955. The very edges of the two profiles obtained near the skeleton surface indicate unusually high lead contents (1.39 µg/g and 3.37 µg/g) with respect to those measured in other samples described below for the same period. In the last growth layers, preliminary synchrotron tomographies indicate the presence of a porous network, absent in the underlying layers. This

feature could generate abnormally high lead contents (by lead adsorption at the surface of the pores) that are difficult to reconcile with inner values. In the data presented below, care was taken to start or end compositional profiles a minimum of 150 or 200 µm away from the skeleton surface. In the case of the Cap de Creus sample, the values obtained in the layer closest to the skeleton surface were discarded and are not shown in Fig. 3.

The skeleton section in the Medes colony that was collected in 2002 is about 1 cm in diameter and developed over the period 1930-2002. Three LA-ICPMS profiles were obtained and SEM images were assembled to obtain a detailed map of the sample (Figure 4a). Figure 4b shows the 3 profiles, including profile 1 presented as an example in Figure 2. Data have been fitted with a locally weighted least square error method. The data dispersion on both sides of the fitting curve is relatively low (~ ± 0.1 µg/g), except at the maximum concentrations where two values close of 1.2 µg/g depart from the fitted trend shown in red. The three profiles show similar patterns. Starting in 1930, a relatively constant lead content of about 0.3 ± 0.1 µg/g is observed and continues to about 1952. After 1952, lead concentrations increase rapidly at first (1952-1960), then more slowly (1960-1970), then increase rapidly again (1970-1980) to reach a maximum of about 0.7 µg/g at the end of the 1970s. This sample confirms that the increase of lead concentration began during the period 1952-1958 as is also observed in the Cap de Creus sample. From 1980 to 2000, the lead contents in Medes 2002 decreases to reach values close to or slightly below those measured in 1930 (mean value calculated within the interval 1998-2002: 0.26 ± 0.01 µg/g).

Another sample collected at the same location in 2014 (Medes 2014) provides additional data for the period 1974-2014 (Figure 5). The data confirm the decrease of lead content between 1980 and 2000 and indicates a stabilization of the lead concentrations at about 0.25 µg/g for the period 1998-2014.

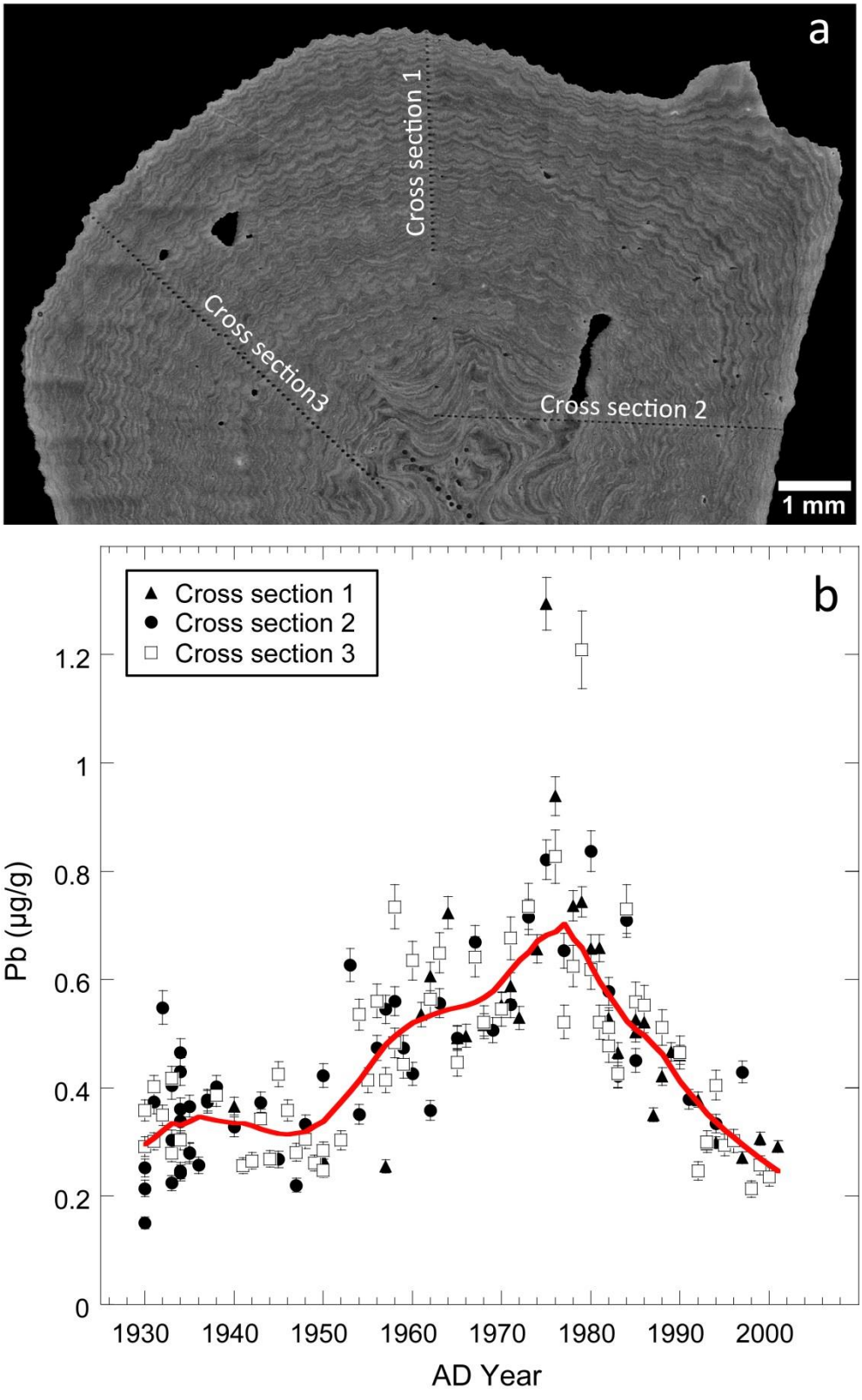

Figure 4: *Lead profiles in Medes samples. a) Mosaic of SEM images of a coral collected in the Medes Islands in 2002. The black dots represent the spots of the LA-ICPMS analyses and mark the locations of the three profiles. b) Pb contents along the 3 profiles. Data have been fitted using a locally weighted least square error method (red curve).*

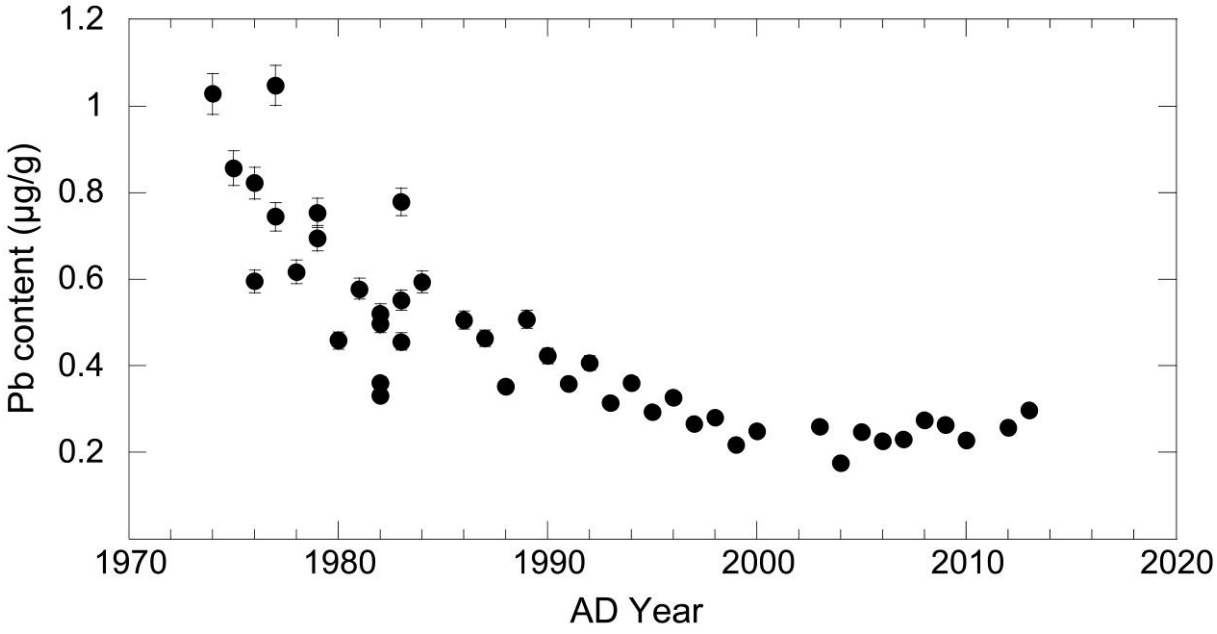

***Figure 5**: Pb profile obtained in a sample collected at Medes in 2014*

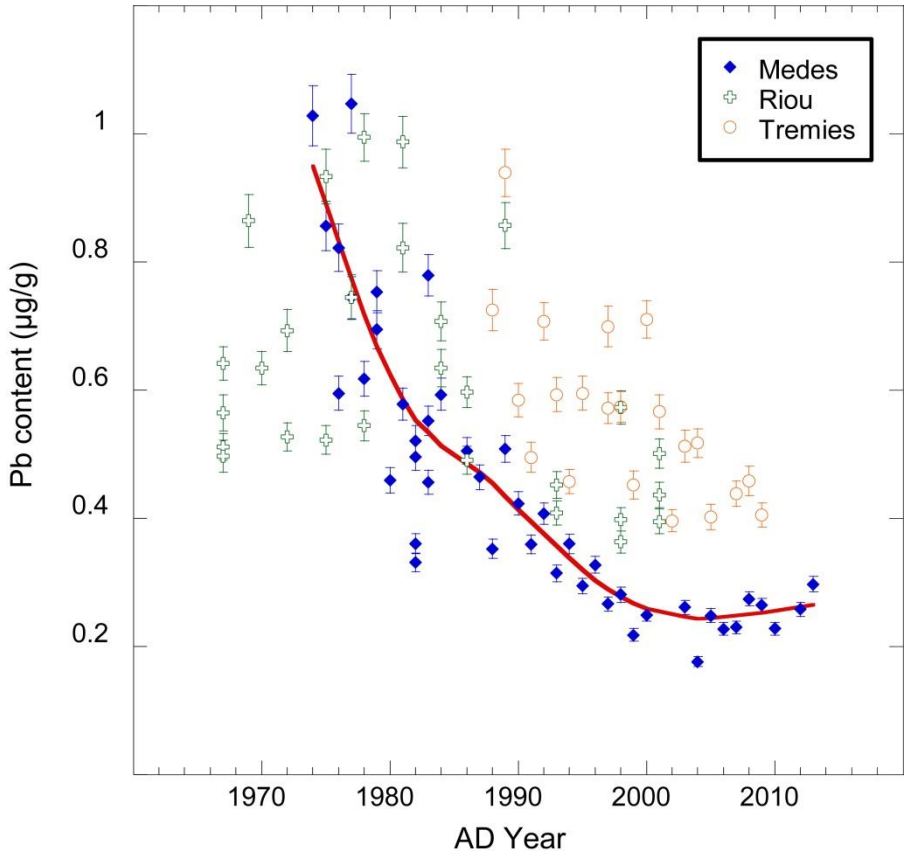

Figure 6: Pb profiles in 3 different colonies recently collected near the Medes Islands, Riou Island, and Tremies cave in 2014, 2002 and 2010, respectively. Riou Island and Tremies cave are close to Marseille, a highly populated area. The Medes data have been fitted using a locally weighted least square error method.

The data obtained from three coral skeletons collected at different locations (Riou 2002, Medes 2014, Tremies 2010) are compared in Figure 6. Although the concentrations differ, a decrease of Pb content with time is observed in all samples. After 1980, the red coral from Medes 2014 shows lower Pb contents than the two others. The differences are interpreted in terms of local effects related to geology, river inputs, or human activity including lead mining and processing activities.

Data obtained on *C. rubrum* samples from Italy and Algeria collected after 2010 are listed in Table 2 as supplementary materials. The mean lead compositions vary between 0.11 and 0.43 µg/g. The significance of these variations will be discussed below.

To summarize, the lead concentrations in *C. rubrum* skeletons show systematic variations with time. Constant concentrations of about 0.2-0.3 µg/g are observed during the period 1890-1954, followed by an increase during the period 1954-1978, to reach a maximum at about 0.8 µg/g in 1978 ± 2 years, and then a progressive decrease to ~0.25 µg/g in 2000. The period 2000-present is marked by a relatively constant lead concentration of about 0.25 µg/g. Local anthropogenic and natural effects influence the concentrations of lead in present-day skeletons.

3.2 Lead contents in sub-fossil C. rubrum skeletons from the Mediterranean

In order to study the anthropogenic impact on the environment, it is important to determine the reference level of lead concentration in the red coral before the development of human activities. This is a difficult task as lead pollution associated with human activities started ~5,000 years ago (Settle and Patterson, 1980). The sample collected in the sedimentary layers of the Tremies Cave is about 2,000 year old which means that this colony grew during the Roman period. Since then, it was buried in sediments. While the inner part of the skeleton kept its original red color, the outer part became dark as a consequence either of the

311 degradation of organic matter or the presence of manganese and iron oxide deposits
312 commonly found in shallow and dark submarine caves (Allouc and Harmelin, 2001).

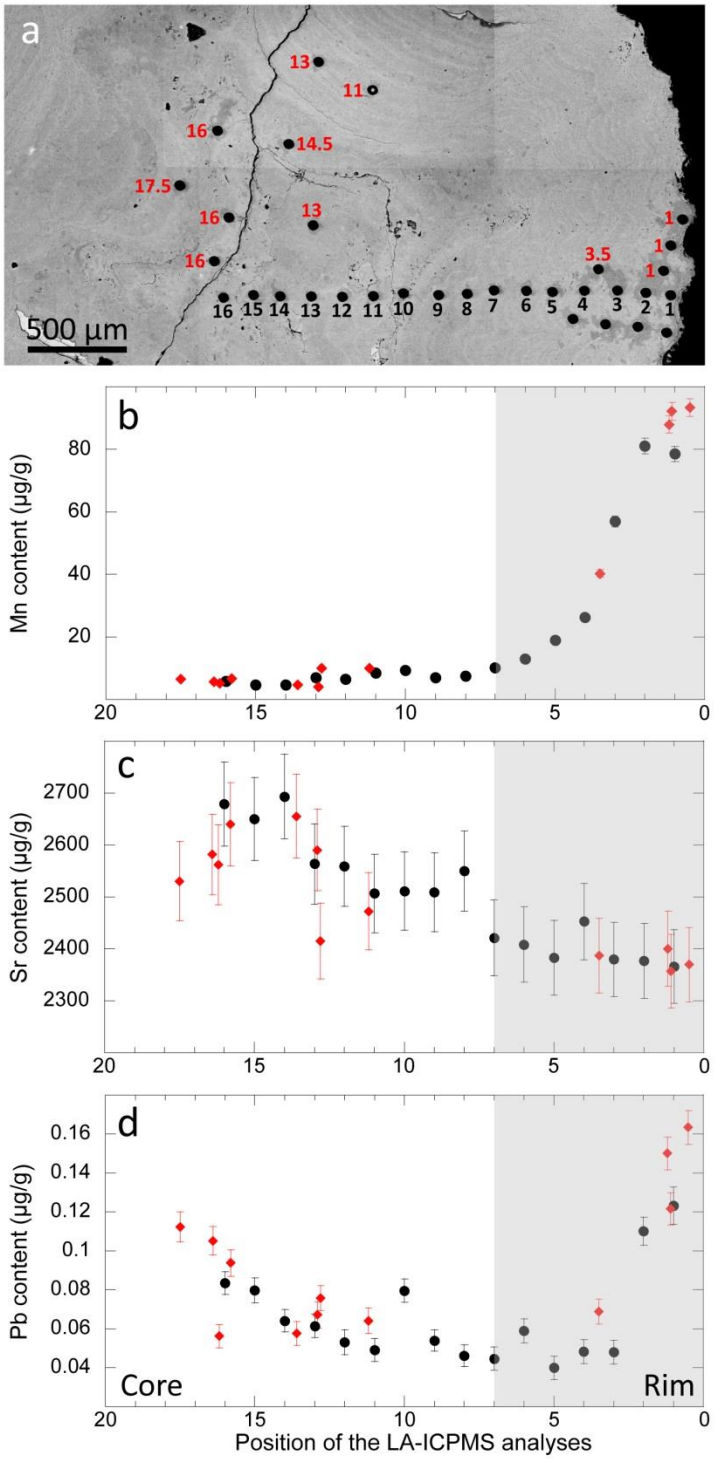

313

314 ***Figure 7****: Two thousand year old sub-fossil sample. a) SEM image of the sample collected in*
315 *the sediments of the Tremies Cave and location of the LA-ICPMS spots (black numbers for*
316 *the spots along the profile and red for spots elsewhere). b), c) and d) Mn, U, and Pb*
317 *concentrations along the lead profile.*

The interior of the skeleton displays the same crystallographic organization as present-day skeletons (as determined byVielzeuf et al., 2010) when observed with optical microscope or SEM (see Fig. 7a). X ray diffraction analysis of this skeleton shows no difference when compared to present day corals. Some elements display gradients in concentration from rim to core of the skeleton. Magnesium and strontium increase slightly (Figure 7c). The largest difference is observed with manganese, which decreases from ~80 µg/g to ~7 µg/g towards the center (Figure 7b). It should be noted that even in the core, the Mn concentrations are larger than in the present-day *C. rubrum* skeletons (~7 compared to ~1.5 µg/g – Vielzeuf et al 2018). To a lesser extent, uranium follows the same trend from core to rim but concentrations in the core are similar to those observed in present-day *C. rubrum* (~0.08 µg/g). These observations, in particular the high concentrations of manganese, are attributed to diagenetic mobilization of Mn from within the sediments (Brand and Veizer, 1980; Gillikin et al., 2005; Kaufman et al., 1996). Concerning lead, the concentrations close to the rim (~0.14 µg/g) are higher than those in the interior of the skeleton. To determine a mean lead content of *C. rubrum* in the pre-industrial period, analyses close to the edge were discarded (Figure 7d – the grey area) and the value of 0.07 ± 0.02 µg/g for Pb concentration is obtained.

The Sciacca corals provide another opportunity to determine a background level of lead in the corals prior to extensive human activities. A sample of Sciacca coral was analyzed at LMV; it showed lower concentrations in sodium, phosphorus, potassium, and higher concentrations in manganese (41 ± 10 *vs* 1.4 ± 0.3 µg/g) and uranium (0.14 ± 0.02 *vs* 0.06 ± 0.02 µg/g) than present-day *C. rubrum* skeletons (supplementary materials, Table 2). Concerning Mn, no concentration gradient was observed. Lead contents increased close to the edge of the sample but reached a plateau inside the skeleton. Discarding some values at the

342 edge of the sample, a value of 0.09 ± 0.01 µg/g was obtained for lead contents in these ancient
343 *C. rubrum* skeletons.

344 As stated above, another set of Sciacca and present-day *C. rubrum* skeletons were
345 analyzed at Virginia Tech (VT) (Supplementary materials – Table 3). The Sciacca samples
346 dated ~2100-2400 BP and ~4050-4400 BP represent times before the widespread introduction
347 of Pb into the environment through human activities. Interestingly, the mean concentrations
348 measured on present-day corals in this dataset are remarkably consistent with those
349 determined by Vielzeuf et al. (2018), except for K and Zn that show slight differences. In the
350 VT dataset, compared to present-day corals, the sub-fossil samples are enriched in Mn (48 ±
351 17 *vs* 0.9 ± 0.5 µg/g), Fe (172 ± 107 *vs* 0.69 ± 0.04 µg/g), Cu (1.6 ± 1.6 *vs* 0.15 ± 0.02 µg/g),
352 and U (0.26 ± 0.15 *vs* 0.08 ± 0.04 µg/g). These high concentrations can be attributed to
353 diagenetic processes as will be discussed below. An important question is to determine
354 whether the lead contents are also affected by diagenetic transformations. In the Sciacca
355 compositions listed in Table 3 (supplementary materials), two groups can be distinguished on
356 the basis of Mn and Fe concentrations, with cutoff limits at 50 and 150 µg/g for Mn and Fe,
357 respectively. The highest Fe and Mn concentrations are observed in the oldest samples (4050-
358 4400 BP). No change of lead concentration is observed between these two groups. Thus, the
359 impact of diagenesis on lead concentrations seems to be limited and a value of 0.10 ± 0.03 is
360 retained as the original content of lead in these corals.

361 Considering the three types of sub-fossil samples (Tremies cave 2000, Sciacca LMV,
362 Sciacca VT), a mean value of 0.09 ± 0.03 µg/g will be taken as the lead concentration in sub-
363 fossil *C. rubrum* skeletons from the Mediterranean, keeping in mind that the lowest lead
364 contents measured are ca 0.04 µg/g, and that natural local effects (geology hydrology, marine
365 currents) can also affect the original lead concentrations in these corals.

366 *3.3. Coralliidae from other oceans*

Corallium rubrum and other Coralliidae from the Atlantic Ocean

Previous comparative studies of *Corallium* species from the Mediterranean, Atlantic and Pacific Oceans showed that the mineralogy, crystallographic structure, overall chemical compositions, and skeleton growth modes are similar (Perrin et al., 2015). This similarity justifies a comparison of their lead contents and allows covering a larger geographic area than the Mediterranean alone.

Compositional profiles obtained on two samples of *C. rubrum* from the southern coasts of Portugal collected in 2012 do not show compositional variations; their mean concentrations is 0.22 ± 0.06 µg/g, close but slightly lower than the lowest values recorded in the Medes 2014 sample for the period 1998-2014. The main difference between the Portugal and Medes samples is that the first ones do not show lead content decrease in the profile, meaning that the lead content had been almost constant in these corals for the last ~25 years.

Samples of *C. johnsoni* from the Azores islands collected in 2011 show no lead concentration variations along two ~3000 and ~4000 µm long traverses. The mean lead concentration in *C. johnsoni* is low: 0.10 ± 0.03 µg/g. The results obtained on *C. niobe* from the same location in the Atlantic are remarkably similar, with a mean lead concentration of 0.11 ± 0.03 µg/g, along a 5500 µm diametral traverse.

Coralliidae from the Pacific Ocean

Pacific Ocean samples of *C. japonicum* and *C. konojoi* were analyzed from rim to core but no SEM observation was carried out to identify and count the growth rings. Concerning the *C. japonicum* sample collected in 2013, no variation was observed along a ~1800 µm long traverse. However, with a mean of 0.16 ± 0.04 µg/g, lead concentrations are higher than in the Azores corals from the Atlantic. Similar conclusions apply for a 2700 µm-long traverse in *C. konojoi* collected in 2015, with a mean concentration of 0.17 ± 0.03 µg/g. Considering a growth ring width of about 150 µm year^{-1}, these traverses indicate that no significant change

of lead concentrations occurred during the last 10-20 years preceding their sampling in the Pacific. The mean Pb concentrations of all studied samples are given in Table 1 (main text) and in Tables 2 to 4 (supplementary materials). Lead contents along different profile are provided as supplementary materials in Table 5.

		Pb (µg/g) mean content	SD (µg/g)	n	Range of Pb concentrations	units
C. rubrum	***Calcite***					
Tremies 2000 year old		0.07	± 0.02	18	0.05 - 0.11	µg/g
Tremies 2010		0.61	± 0.15	27	0.40 - 0.94	µg/g
Cap de Creus 1962		0.17	± 0.09	75	0.07 - 0.71	µg/g
Medes 2002		0.46	± 0.18	146	0.15 - 1.29	µg/g
Profile 1		0.51	± 0.21	35	0.26 - 1.29	µg/g
Profile 2		0.42	± 0.16	52	0.15 - 0.84	µg/g
Profile 3		0.45	± 0.18	59	0.21 - 1.21	µg/g
Medes 2014		0.46	± 0.22	44	0.18 - 1.05	µg/g
Riou 2002		0.61	± 0.20	27	0.36 - 0.99	µg/g
Other *Coralliidae* (octocorals)	**Calcite**					
C. niobe 2005 (Azores)		0.12	± 0.05	14	0.06 - 0.28	µg/g
C. johnsoni 2011 (Azores)		0.11	± 0.04	25	0.06 - 0.23	µg/g
C. japonicum 2013 (Japan)		0.15	± 0.03	22	0.10 - 0.19	µg/g
C. konojoi 2015 (Japan)		0.16	± 0.03	25	0.12 - 0.21	µg/g
Litterature data						
Desenfant et al. (2006)		0.04	± 0.02	84	0.02-0.08	µg/g
Mona Island coral (*Montastraea faveolata*)	**Aragonite**				9 - 40	nmolPb/molCa
Sinclair et al. (2011) Bamboo coral (*Keratoisis sp.*) from SE USA	**Calcite**				~ 0 - 0.14	µg/g
Inoue et al. (2006) Porites coral from Japan	**Aragonite**				~ 0.01 - 0.07	µg/g
Kelly et al. (2009) John Smiths Bay - *D. labyrinthiformis*	**Aragonite**				4 - 65	nmolPb/molCa
North Rock - *D. strigosa*	**Aragonite**				6 - 31	nmolPb/molCa
North Rock - *D. labyrinthiformis*	**Aragonite**				30 - 80	nmolPb/molCa

Table 1 *- Lead content of some calcitic Corallium skeletons and other calcitic or aragonitic corals.*

Summary of the observations:

(1) Lead concentrations in *C. rubrum* skeletons from the Mediterranean are stable for the period 1894-1955 and are within the range 0.2-0.4 µg/g; concentrations increase up to about 1-1.2 µg/g during the period 1960-1978, then decrease progressively to stabilize and reach values in the range 0.2-0.4 µg/g in present-day corals.

(2) Sub-fossil Mediterranean *C. rubrum* are enriched in Mn, Fe, Cu and U, and depleted in Sr, Na and Mg, in comparison to present-day *C. rubrum*. Their lead concentrations are ~0.09 ± 0.03 µg/g.

(3) Lead concentrations in the Pacific *C. japonicum* and *C. konojoi* are lower than in the Mediterranean *C. rubrum*, with values close to 0.17 ± 0.03 µg/g.

(4) The lowest lead concentrations in present-day samples are found in two *Corallium* species from the Azores islands in the Atlantic (0.11 ± 0.03 µg/g).

4. Discussion

4.1 Lead in biogenic carbonates

The content of Pb in *Corallium rubrum* skeletons can be compared with other octocorals (calcite skeleton) or hexacorals (aragonitic skeleton) (Table 1 and references therein). Sinclair et al. (2011) reported a maximum Pb content of about 0.13 µg/g in the deep-water bamboo octocoral *Keratoisis sp.*, at least 2 times lower than in the red coral. Lead contents in scleractinian corals made of aragonite reported by Shen and Boyle (1988), Desenfant et al. (2006) and Kelly et al. (2009) are within the range 0.01-0.2 µg/g, *ca* an order of magnitude lower than those recorded in *Corallium* skeletons made of high magnesium calcite. For example, Desenfant et al. (2006) observed a peak in Pb content along a profile in Mona Island hexacoral skeletons at about 0.08 µg/g whereas a peak is observed at 1-1.2 µg/g in the Mediterranean *C. rubrum* for the same period. This is not necessarily an expected result considering that the calcium cation site that may accommodate the larger Pb cation is larger in aragonite than in calcite. Thus, the aragonite structure accommodates Pb substitution more easily, which is consistent with the fact that $PbCO_3$ (cerussite) forms an isostructural solid solution with aragonite. How can we explain this apparent inconsistency? The LA-ICPMS analyses of lead in *Corallium* species presented here have been carried out in three different laboratories (ETH-Zurich, Switzerland; Virginia-Tech, USA; and LMV Clermont-Ferrand, France) on similar samples and the results are consistent. For this reason, an error greater than 50% relative for our measured lead concentrations is excluded. Also, the interpretation that Pb cannot enter the calcite structure does not hold if the case of Sr, with an effective ionic radius

(IR) similar to the radius of Pb is considered [IR_{Ca} = 1.0Å, IR_{Pb} = 1.19Å, IR_{Sr} = 1.18Å, in sixfold coordination, (Shannon, 1976)]. Indeed, large amounts of Sr (*ca* 3000 µg/g) are incorporated into *Corallium* high magnesian calcites (Hasegawa et al., 2010; Vielzeuf et al., 2018; Vielzeuf et al., 2013; Weinbauer et al., 2000). Finally, it should be noted that *Corallium* biogenic calcites are defective crystalline structures both from a structural (Perrin et al., 2015) and chemical point of view. The incorporation of cations like Mg, Sr, Na and organic matrix promotes the formation of defects in calcite, and this in turn, may allow calcite to accommodate lead in its structure. The difference in lead concentrations in aragonitic and calcitic *Corallium* species may not be a result of structural differences but, rather, may reflect varying availability of lead in the seawaters in which the corals are growing. Another possibility suggested by Rosenheim et al. (2005) to explain lead concentration differences between sclerosponge aragonite and aragonite from zooxanthellate corals (10 times more Pb in sclerosponges) is that pumping and filtering seawater and particulates is the only source of nutrition for *Corallium* species, while zooxanthellate corals receive additional nutrients from their algal symbionts. Nevertheless, except in the Mediterranean where the lead contents in *C. rubrum* can be high and close to 1.2 µg/g, concentrations in *Corallium* from the Atlantic and the Pacific are rather low and closer to the values measured in aragonitic corals in the above-mentioned studies.

At this stage, it is worth mentioning that *Corallium* species incorporate significant amounts of organic matrix (between 20,000 and 40,000 µg/g (Allemand, 1993; Vielzeuf et al., 2018). In scleractinian corals, it is generally agreed that lead is preferentially concentrated in coral tissues relative to skeletons (Barakat et al., 2015; Esslemont, 2000; McConchie and Harriott, 1992). To our knowledge, lead contents in octocorals tissues have not been studied so far, but a similar tendency can be expected. Thus, some lead could be associated with the organic matrix in *Corallium* skeletons. Though this hypothesis cannot be discarded, this is not

458 our preferred interpretation. Indeed, no difference in lead concentration is observed between
459 medullar and annular zones of *C. rubrum*, in spite of the fact that the medullar zone is 10 wt%
460 richer in organic matrix than the annular zone (Vielzeuf et al., 2018). In addition, a fossil *C.*
461 *rubrum* of upper Pliocene age (Giampilieri, Province of Messina, Sicily), not included in the
462 present study because of intense chemical transformations with total loss of organic matrix
463 and ~75% loss of magnesium, shows lead concentrations of about 0.3 ± 0.2 µg/g
464 (supplementary materials – Table 2). These values cannot be taken as original lead contents in
465 these *C. rubrum* skeletons, *ca* 2 million year ago, but they show that lead can be present in
466 calcite that is devoid of organic matrix.

467 Following on earlier work on lead in aragonitic or calcitic corals (Esslemont, 2000;
468 Hanna and Muir, 1990; Shen and Boyle, 1987), three hypotheses can be considered for the
469 incorporation of Pb in *Corallium* skeletons: (1) adsorption on skeleton surfaces (or pore
470 surfaces), (2) lead binding by organics in the organic matrix, and (3) substitution of lead in the
471 calcite structure. The unusual high lead contents close to the surface of *Corallium* skeletons
472 (last growth rings) described above can be attributed to option (1) and data from the last
473 growth rings were discarded from lead traverses. Inside the skeleton, this hypothesis is
474 discarded due to the density of the inner skeleton. The hypothesis of organically bound lead
475 (2) cannot be discarded, but is difficult to verify and quantify. In our opinion and for reasons
476 given in a previous paragraph, the most plausible origin for the presence of lead in *Corallium*
477 skeletons is Pb cations substituting in the cation site (option 3).

478 4.2 Significance of lead concentrations and diagenetic indicators in sub-fossil corals

479 The quest to determine lead contents in *Corallium* skeletons that developed prior to recent
480 human impact led to the study of sub-fossil corals. As seen above, contents of Mg, Sr, and Na
481 are lower in sub-fossil corals than in present-day corals, while contents of Mn, Fe, Cu are
482 higher. These are expected features in carbonates that underwent early diagenetic

483 modifications (Brand and Veizer, 1980; Swart, 2015; Ullmann and Korte, 2015). The case of
484 elements with multiple oxidation states is interesting. As stressed by Ullmann and Korte
485 (2015) manganese and iron concentrations are low in oxygenated seawaters because they
486 precipitate as oxy-hydroxy phases (Crerar and Barnes, 1974; Glasby and Schulz, 1999). As a
487 consequence, Fe and Mn concentrations are low in biogenic calcites. Under reducing
488 conditions such as might occur in organic-rich sediments, the oxidation state of these
489 elements can change and Mn and Fe can enter the calcite structure (Brand and Veizer, 1980;
490 Thomson et al., 1986). Indeed, isostructural solid-solutions exist between calcite,
491 rhodochrosite ($MnCO_3$), and siderite ($FeCO_3$). The status of U in carbonates during diagenesis
492 is not so well documented. The difference between present-day and sub-fossil corals favors an
493 enrichment of U during diagenesis. Concerning lead, a main question that remains is whether
494 lead concentrations in *C. rubrum* are affected by diagenesis. Figure 7 indicates that lead
495 concentrations increase at the edge of the coral skeleton. By analogy with Mn content, this
496 increase could be interpreted in terms of progressing diagenetic transformation. However, it
497 could also be interpreted as a rim effect as observed in present-day samples. The diagenetic
498 effect on the concentration of lead could thus be minimal, which is in agreement with the fact
499 that lead concentrations in the Sciacca corals are still low compared to present-day corals.

500 4.3 Interpretation of lead variations in *Corallium* skeletons

501 The present study answers the question of the origin of the large variation of lead content
502 observed in *C. rubrum* skeletons by Vielzeuf et al. (2018): lead contents depend on the date
503 and place of coral growth.

504 *4.3.1 Temporal variations in lead content in Corallium skeletons*

505 Five stages can be considered for the evolution of lead content in *C. rubrum* with time: (1) a
506 pre-industrial content in the two thousand years and older samples (Fig. 7), (2) a plateau for
507 the period 1895-1955, possibly with a slight decrease during the period 1905-1930 (Figs 3 and

8), (3) a sharp increase starting in 1955 and reaching a peak in 1974-1980, possibly with a shallower slope for the period 1962-1970 (Figs 4 and 8), (4) a sudden decrease tending toward a lower plateau during the period 1977-2000 (Figs 5, 6 and 8), and (5) lead contents close to pre-1955 values after 2000 (Figs 5 and 6).

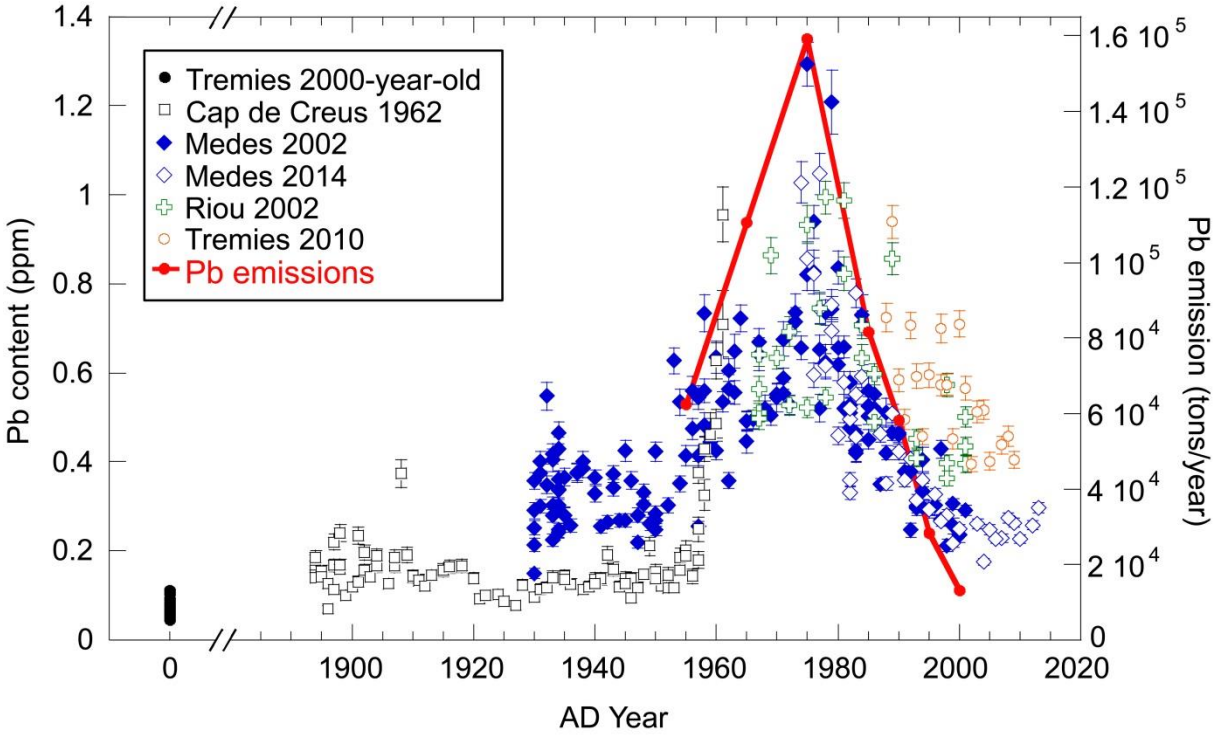

***Figure 8**: Summary of Pb profiles obtained in this study. Pb emissions recorded in Europe from 1955 to 2000 are reported for comparison (Pacyna et al., 2007; Pacyna and Pacyna, 2000).*

It is important to note that the pre-industrial value determined above in red coral skeletons (in the range 0.04-0.1 µg/g) cannot be necessarily taken as pre-anthropogenic concentrations as different studies point out that lead contamination already existed 2,000 years ago due to lead mining and production during the Roman Empire and earlier (Nriagu, 1998; Shotyk et al., 1998). Indeed, the use of lead in human civilization appeared very early, *ca* 6400 B.C. (Wertime, 1973) and the first noticeable trace of human lead pollution dates back to the late Bronze Age (~1200 B.C.) (Hong et al., 1994; Martinez-Cortizas et al., 1997; Shotyk et al., 1998). It should also be noted, however, that one of the Sciacca samples was

525 formed ~4050-4400 BP and pre-dates the earliest anthropogenic lead pollution, and this
526 sample contains ~0.1 µg/g Pb. Since the pioneering work of Clair Patterson and his group at
527 Caltech, it is well established that the use of leaded gasoline for better functioning of car
528 engines that started in 1923 in the USA and soon thereafter throughout the world had a
529 noticeable impact on the environment at a global scale (Murozumi et al., 1969; Patterson,
530 1965). These observations initiated a change of regulation and the USA started reducing the
531 lead concentration in gasoline though the adoption of new policies during the mid-1970s (see
532 Nriagu (1990) for a review). In European countries, restrictions on the lead content in
533 gasoline were gradual and finalized by the EU-regulation in 1989 and the Aarhus Treaty
534 signed in 1998 (von Storch et al., 2003). The cycle of lead increase and decrease covering the
535 period 1955-2000 in red coral skeletons (Figure 8) is an illustration of a pollution crisis
536 referred to as the 'lead gasoline anomaly' below. The total Pb emissions in Europe during the
537 period covered by the coral record (Pacyna et al., 2007; Pacyna and Pacyna, 2000) is plotted
538 in Fig. 8 for a comparison. By averaging the lead contents in the red coral skeletons during the
539 period (1955-2000), i.e. when Pb emissions in Europe are available, a linear (Pearson) cross-
540 correlation coefficient between Pb content in the coral skeleton and Pb emissions in Europe of
541 0.87 is observed ($p = 0.01$). Thus, the variations in lead contents in coral samples are well
542 correlated with variations of lead atmospheric inputs from Europe (Figure 8). The lead
543 profiles in the red coral are also in agreement with reconstruction of anthropogenic lead
544 emissions in France where the flux suddenly increased in ~1950, decreased progressively
545 during the period 1970-1985, and rapidly after that, as shown by Ferrand et al. (1999) in their
546 Figure 8.

547 The lead pollution cycle, or parts of it, has been registered in different contexts. Ice
548 core profiles in central Greenland show an increase in lead content during the period ~1880-
549 1910, followed by a decrease for the period ~1910-1940, a new increase for the period 1930-

1970, and a decrease in the interval 1970-2000 (Boutron et al., 2004; McConnell et al., 2002). In the red coral profiles, the slight decrease during the period 1905-1930 could match the decrease observed in ice records. This trend is also recorded in reconstructed atmospheric deposition in sediments from Spain (Corella et al., 2017). In Greenland ice records, the lead gasoline anomaly starts earlier than in the red coral (1935 *vs* 1955). This difference could reflect a better sensitivity of ice than corals to record lead pollution. The pollution peak during the lead gasoline anomaly is also slightly different (1970 in ice cores *vs* 1974-1980 in the red coral). This could be attributed to earlier application of lead regulation in the US than in countries around the Mediterranean. It will be noted that this decrease is in good agreement with the decrease in lead concentrations observed in leaves and human blood for the same period (von Storch et al., 2003). Finally, the return to a level prior to the use of leaded gasoline is well marked in the red coral (Figs 5 and 6). This pattern is consistent with the return of lead emissions in Europe to pre-1950 levels in the years 2000 (Miralles et al., 2006; von Storch et al., 2003).

Studies on Pb contents in scleractinian coral skeletons also show lead variations during the last decades in western North Atlantic areas (Kelly et al., 2009; Shen and Boyle, 1987) as well as in the western Pacific Ocean (Inoue et al., 2006), Caribbean Sea (Desenfant et al., 2006) and Indian Ocean (Lee et al., 2014). Records of lead pollution in other marine organisms, such as Bamboo corals (Sinclair et al., 2011), sclerosponges (Lazareth et al., 2000) and clams (Gillikin et al., 2005) are also available (see Shotyk and Le Roux (2005) for a review). Figure 9 shows a comparison of Pb concentrations of the calcitic red coral skeletons and three other aragonitic coral skeletons (Desenfant et al., 2006; Kelly et al., 2009) during the last century. Even if Pb concentrations are different in the different corals, identical trends are generally observed. However, it has been shown that the timing of the event can vary

574 significantly from one place to another, especially in the Indian Ocean (Lee et al., 2014),
575 probably due to differences in the timing of application of new regulations.
576 *4.3.2 Spatial variations in lead content in Corallium skeletons*
577 As discussed above, lead contents in precious *Corallium* species from the Mediterranean, the
578 Atlantic and the Pacific differ, probably indicating different levels of lead in the seawaters.
579 The Atlantic *C. rubrum* contains less lead than its Mediterranean analogue [mean value of
580 0.23 +/- 0.06 compared to 0.48 +/- 0.19 µg/g (Vielzeuf et al., 2018)] and does not show a
581 significant decrease for the period 1992-2012. We ascribe this difference to lead content
582 differences between the Atlantic Ocean and the Mediterranean Sea, as will be discussed
583 further below. More locally, the comparison of *C. rubrum* samples from different locations in
584 the Mediterranean for the period 1980-2010 (Figs. 6 and 8) indicates that the trends of
585 decreasing lead contents are identical but that the absolute values differ: the Medes 2014
586 sample displays the lowest contents, while Riou 2002 and Tremies 2010 (sampling sites
587 separated only by about ten kilometers) have similar contents. Differences can be explained
588 by the presence of ancient lead processing factories in the Marseille area (Daumalin and
589 Raveux, 2016) which locally contaminate the seawater (Laffont-Schwob et al., 2016). These
590 observations indicate that the red coral is sensitive to the overall pollution but also records
591 local effects. In particular places, red coral could be used to monitor the evolution in time of
592 specific anthropogenic lead pollutions. Here again, the situation is similar in scleractinian
593 coral, as Medina-Elizalde et al. (2002) showed differences of lead contents in the skeleton of
594 *Orbicella annularis* (formerly named *Monstastraea annularis*) from two distinct areas,
595 Cancún and Majahual, located about 300 km from each other. The Cancún area showed a
596 more important lead pollution due to its rapid human development.
597

598 4.4 Comparison with other lead records in the Mediterranean

599 In the western Mediterranean region, data acquisition of seawater and atmosphere Pb contents
600 started in the early 1980s and showed a decrease of Pb atmospheric concentration at the end
601 of the 1980s, delayed with respect to North America (Annibaldi et al. (2009); Migon et al.
602 (2008) and reference therein). This delay can be attributed to differences in the timing of
603 implementation of lead gasoline regulations between Europe and the USA.

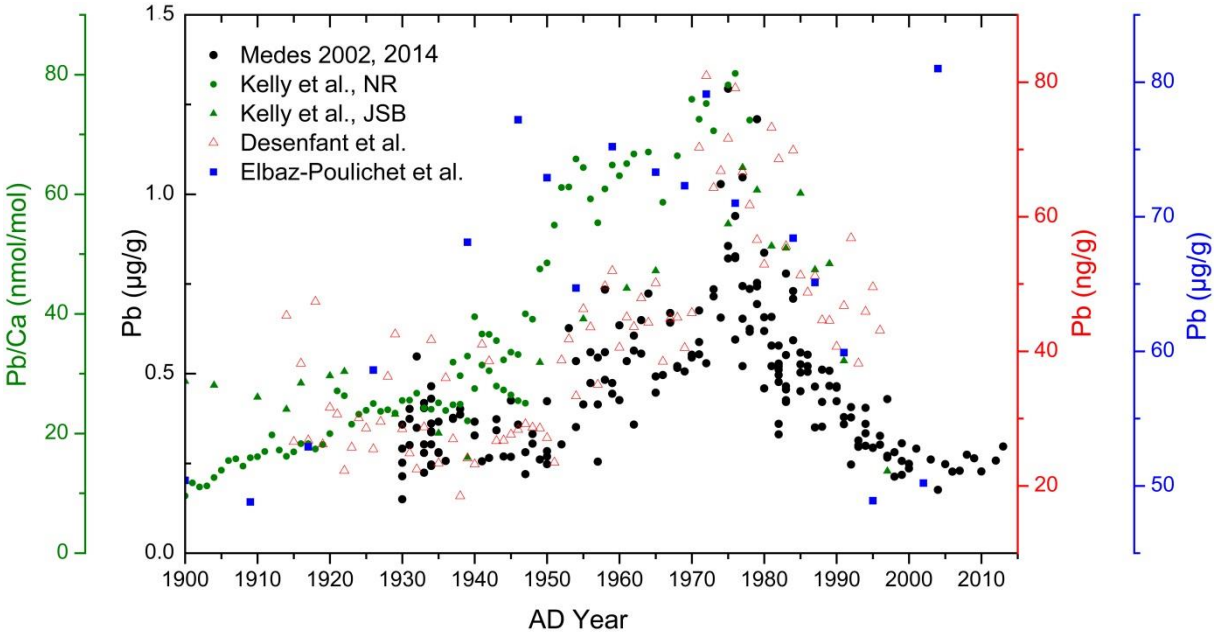

604

605 ***Figure 9****: Pb concentration profiles obtained in Medes 2002 and 2014 (black dots) compared*
606 *with other records (green dots and triangles: two scleractinian corals from the Atlantic*
607 *Ocean (Kelly et al., 2009); red triangles: massive coral from the Caribbean Sea (Desenfant et*
608 *al., 2006); blue squares: sediment core from the Northwestern Mediterranean Sea (Elbaz-*
609 *Poulichet et al., 2011). The color of the Y-axis match the different datasets.*
610

611 Although the measurement of Pb concentration in seawater and atmosphere is an effective
612 method to evaluate inputs of anthropogenic Pb, temporal records of Pb concentration are
613 limited. The current status of specific regional pollutions by metallic contaminants in the
614 Mediterranean basin has been the subject of studies using sea plants, mussels, seawater or
615 sediments (e.g., (Gosselin et al., 2006; Mikac et al., 2015; Serrano et al., 2011; Tranchina et
616 al., 2005). Mussels and sea plants are indicators of present-day local pollution in the
617 Mediterranean basin (Casas et al., 2008; Gosselin et al., 2006). However, such organisms do

not record lead variation over long periods of time, even if a correlation between lead concentrations in a sea plant (*Posidonia oceanica*) and estimated lead emissions in the same area is observed (Tranchina et al., 2005). Some studies provide lead profiles in Mediterranean sediment cores (Elbaz-Poulichet et al., 2011; Miralles et al., 2006). The Pb concentrations determined by Elbaz-Poulichet et al. (2011) are plotted in Figure 9. Corals and sediments display similar trends but the sediment peak is wider. This difference can be explained by possible disturbances associated with remobilization and bioturbation processes. Thus, sediment cores provide information on lead contents covering several centuries. Nevertheless, their temporal resolution is not as good as the annual resolution obtained with corals.

4.5 Lead contents in seawater

Data compiled by Annibaldi et al. (2009) give indications of relative lead contents in the Pacific, Atlantic and Mediterranean; lead contents are lower in Pacific and Atlantic seawaters than in the Mediterranean (0.05±0.03, 0.07±0.06, and 0.19±0.11 nmol/L, respectively; means of values tabulated in Annibaldi et al. (2009) – Table 5). A decrease of lead content in surface seawaters in the western North Atlantic Ocean starting in the mid-1980s has been observed and correlated to the leaded gasoline phase out in the USA (Wu and Boyle, 1997). Figure 10 shows Pb concentrations in Mediterranean and Atlantic seawaters (Kelly et al., 2009; Nicolas et al., 1994), together with lead contents in aragonitic corals *Diploria labyrinthiformis* and *D. strigosa* from Kelly et al. (2009), and calcitic *C. rubrum* from the present study. Using Pb concentrations in aragonitic corals and seawaters, Kelly et al. (2009) determined an empirical Pb partition coefficient between aragonite and seawater, defined as $Kd = [Pb/Ca]_{aragonite} / [Pb/Ca]_{seawater}$, ranging from 2.8 to 3.6. These values allowed the authors to infer seawater Pb concentrations before 1979. In the case of *Corallium* species, a new partition coefficient can be proposed. As commonly assumed in this type of calculation (Kelly et al., 2009; Rosenheim et al., 2005), a constant concentration of calcium in seawater ($[Ca]_{seawater}$) of 10.3 mmol/kg

from Bruland (1983) can be used. On another hand, Nicolas et al. (1994) determined Pb concentrations in the Northwestern Mediterranean seawaters ($[Pb]_{seawater}$) for the period 1983 to 1992 ranging from 284 to 176 pmol/kg for the surface layer (10-100 m).

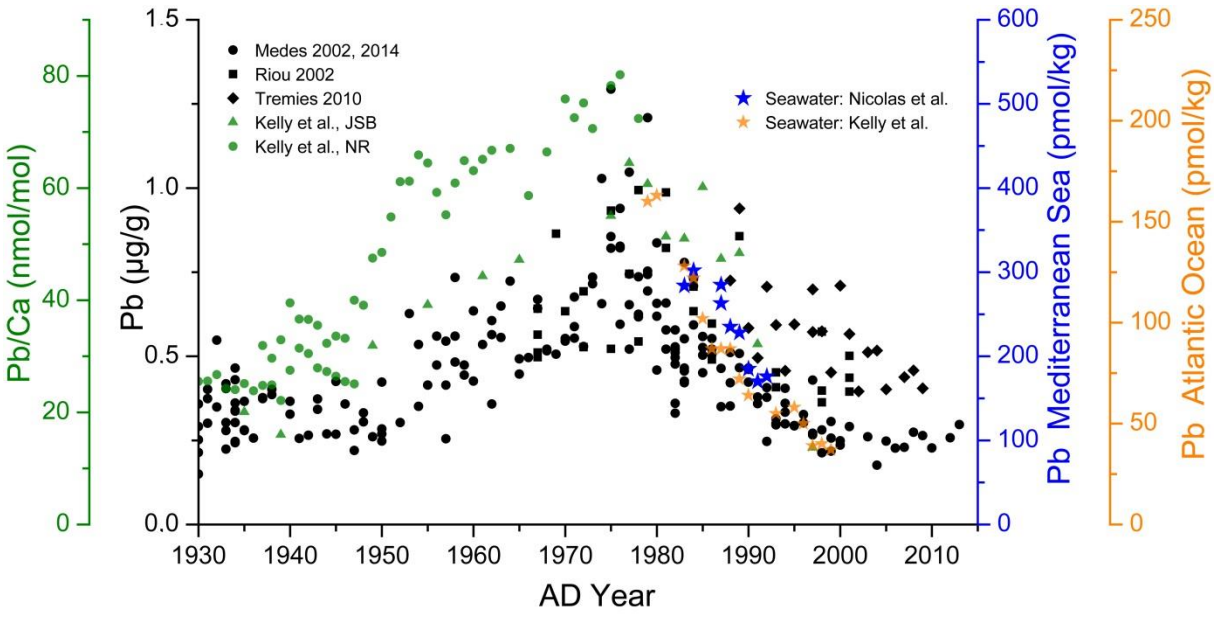

***Figure 10**: Comparison between Pb concentrations in recent red coral skeletons (this study) and Pb concentrations of Mediterranean seawater (blue stars: (Nicolas et al., 1994), and Pb concentrations in two scleractinian corals and in Atlantic seawater (Kelly et al., 2009). Pb concentrations in corals are on the left Y-axes and Pb concentrations in waters are on the right Y-axes*

Using $[Pb]_{calcite}$ and $[Ca]_{calcite}$ of 0.48 and 350,000 µg/g, respectively (Vielzeuf et al., 2018), the calculated partition coefficient varies from 10 to 16. To avoid the uncertainty associated with a calcium content in seawater that depends on salinity, a simpler ratio can be used instead to calculate the lead partitioning: $D = [Pb]_{calcite}/[Pb]_{seawater}$ (concentrations expressed in pmol/kg). Considering lead contents in *C. rubrum* of 0.63 µg/g in 1983, and 0.45 µg/g in 1992 (Fig. 8), D_{1983} and D_{1992} equal 10,706 and 12,340, respectively. A mean D of ~11,500 will be considered as our best estimate. Concerning the *Corallium* species from the Atlantic (Azores Islands), using the lead content in Atlantic seawaters given by Kelly et al. (2009) (Fig. 10) and lead concentrations of 0.11 µg/g determined above, K_d and D are equal to 12.5 and 10,617, respectively, in agreement with partition coefficients determined in the

Mediterranean. These partition coefficients allow us to calculate an approximate Pb concentration of 400 pmol/kg in the seawater of the northwestern Mediterranean during the mid-1970s. The highest values could have reached around 550 pmol/kg at the maximum of the pollution crisis. Table 5 (in supplementary materials) lists some lead contents in present-day *C. rubrum* skeletons, collected in various places in the Western Mediterranean, and in rings that formed after the year 2000. This table shows that lead concentrations still vary depending on location in the Mediterranean. The lowest value at 0.11 µg/g, close to pre-industrial contents, comes from the Montecristo Island, an Italian Natural Reserve since 1971, and one of the least accessible and most protected areas in the Mediterranean Sea (Turicchia et al., 2018). At the opposite, the highest values (Alghero, Sardinia; Marseille area) come from places where lead was historically extracted or processed. Nevertheless, values comprised between ~50 and ~200 pmol/kg remain below the standard values adopted in Italy to guarantee (1) human health over short periods of time, or (2) the defense of the aquatic ecosystem on long terms [720 and 290 pmol/L, respectively - Annibaldi et al. (2011)]. The estimated values of present-day seawater lead contents (Table 5 – supplementary materials) are in good agreement with data from the central Adriatic Sea in 2004 of 130 pmol/L (Annibaldi et al., 2009) and data from the outer Saronikos Gulf, Greece, of 128 pmol/L (median value between 2000 and 2010) (Paraskevopoulou et al., 2014). Nevertheless, some specific areas in the Mediterranean Sea still have high Pb concentrations, such as the Ancona coast of the Central Adriatic Sea [560 pmol/L, (Annibaldi et al., 2011)], or the inner Saronikos Gulf [2600 pmol/L, (Paraskevopoulou et al., 2014)].

5. Conclusion

Various environmental, structural and chemical factors make the red coral and other calcitic *Corallium* species good recorders of lead pollution in the Mediterranean and other oceans. *Corallium* skeletons grow slowly, producing records over long periods of time in a single

colony. The annual character of growth rings is well-established, and rings can be easily identified by non-destructive methods (SEM), allowing the precise positioning (space and age) of *in situ* chemical analyses, and possibly, multiple analyses of a single ring. *C. rubrum* grows at different depths (from the surface to great depths ~1,000 m) allowing the study of large domains in the sea. Precious corals have been used in jewelry since the Neolithic (Skeates, 1993) and ancient corals can be recovered, dated and analyzed in jewels and sediments of different ages. Lead concentrations are high enough to be determined by *in situ* high precision non-destructive methods (LA-ICPMS). Contrary to sediments or ice cores, a partition coefficient of lead between biogenic calcite and seawater can be determined, which allows the seawater lead content during the skeleton growth to be estimated. *Corallium* skeletons can record both local and global effects, and the comparison of skeletons from places with different levels of pollution allows one to separate local effects from global effects. The response of the skeletons to emissions of lead in the environment is fast, probably due to the fact that Pb has a residence time of about 2 years in ocean surface waters (Nozaki et al., 1976).

The studied samples cover the entire cycle of the global lead gasoline pollution event, from the beginning of the impact (in the 1950s) associated with the dramatic increase in the number of cars in the world, to the application of new regulations starting in 1975, and a return to pre-1950 levels in 2000. Twenty-five years of pollution were sufficient to produce Pb levels in seawater that approached values known to endanger human health within short periods of time and certainly endangering the aquatic ecosystem over longer periods of time. A duration similar to that required to reach the pollution peak was required to return to the pre-lead gasoline values. Lead mining and processing sites sustain lead pollution of seawaters over longer periods of time, which emphasizes the need to remediate the industrial sites after the cessation of their activities.

Acknowledgements

This work has been supported by the Agence Nationale pour la Recherche (ANR) through ANR CoRo 2011-2015 and ANR MOBi 2018 and by the Institut National des Sciences de l'Univers (INSU- CNRS) through grant INTERRVIE 2013 to AR and INTERRVIE 2017 to DV. This study benefited from the generosity of numerous contributors who supplied rare samples. We thank P. Raffin and C. Marschal for C. rubrum colonies from various places in the Mediterranean. G. Rajola and Professor Aldo Cinque supplied rare samples to R.J. Bodnar. Red coral samples from the Tyrrhenian Sea were collected thanks to projects financed by the Italian Ministero dell'Ambiente e della Tutela del Territorio e del Mare (Project 2010, Studio di popolazioni di Corallo rosso profondo) and by Ministero delle Politiche Agricole, Alimentari e Forestali (Project 2012, Use of ROV in the management of deep C. rubrum populations). The fossil sample briefly mentioned in the text was provided by H. Zibrowius. Samples of C. japonicum, C. elatius and C. konojoi were kindly provided by S. Tambutté from Centre Scientifique of Monaco, and G. Tanaka from the Precious Coral Protection and Development Association; we thank K. Saiki from Osaka University for initiating the fruitful exchange with G. Tanaka. Rare specimens of C. johnsoni and C. niobe were provided by F. J. de Mora Porteiro from the Department of Oceanography and Fisheries, University of the Azores. Many observations were made on a FESEM financed by the European Fund for Regional Development (EFRD). We thank F. Bedu for his assistance on this instrument. Comments by three anonymous reviewers are gratefully acknowledged. This is contribution ANR MOBi n° 1.

References

Allemand, D., 1993. The Biology and Skeletogenesis of the Mediterranean Red Coral A Review. Precious Corals & Octocoral Research(2): 19-39.

Allouc, J., Harmelin, J.G., 2001. Mn-Fe deposits in shallow cryptic marine environment: examples in northwestern Mediterranean submarine caves. Bulletin De La Societe Geologique De France, 172(6): 765-778.

Annibaldi, A., Illuminati, S., Truzzi, C., Scarponi, G., 2011. SWASV speciation of Cd, Pb and Cu for the determination of seawater contamination in the area of the Nicole shipwreck (Ancona coast, Central Adriatic Sea). Mar Pollut Bull, 62(12): 2813-2821.

Annibaldi, A., Truzzi, C., Illuminati, S., Scarponi, G., 2009. Recent sudden decrease of lead in Adriatic coastal seawater during the years 2000–2004 in parallel with the phasing out of leaded gasoline in Italy. Marine Chemistry, 113(3-4): 238-249.

Barakat, S.A., Al-Rousan, S., Al-Trabeen, M.S., 2015. Use of scleractinian corals to indicate marine pollution in the northern Gulf of Aqaba, Jordan. Environmental Monitoring and Assessment, 187(2).

Boavida, J. et al., 2016. A Well-Kept Treasure at Depth: Precious Red Coral Rediscovered in Atlantic Deep Coral Gardens (SW Portugal) after 300 Years (vol 11, e0147228, 2016). PLoS ONE, 11(2).

Boutron, C. et al., 2004. L'archivage des activités humaines par les neiges et glaces polaires : le cas du plomb. Comptes Rendus Geoscience, 336(10): 847-867.

Brand, U., Veizer, J., 1980. Chemical diagenesis of a multicomponent carbonate system .1. Trace-Elements. Journal of Sedimentary Petrology, 50(4): 1219-1236.

Bruland, K.W., 1983. Trace elements in sea-water. In: Riley J.P., C.R. (Ed.), Chemical oceanography. Academic Press, New-York, pp. 157-220.

760 Casas, S., Gonzalez, J.L., Andral, B., Cossa, D., 2008. Relation between metal concentration in water
761 and metal content of marine mussels (*Mytilus galloprovincialis*): Impact of physiology.
762 Environmental Toxicology and Chemistry, 27(7): 1543-1552.
763 Cattaneo-Vietti, R. et al., 2016. An overexploited Italian treasure: past and present distribution and
764 exploitation of the precious red coral *Corallium rubrum* (L., 1758) (*Cnidaria: Anthozoa*).
765 Italian Journal of Zoology, 83(4): 443-455.
766 Chave, K.E., 1954. Aspects of the biogeochemistry of magnesium 2. Calcareous sediments and rocks.
767 The Journal of Geology: 587-599.
768 Corella, J.P. et al., 2017. 700 years reconstruction of mercury and lead atmospheric deposition in the
769 Pyrenees (NE Spain). Atmospheric Environment, 155: 97-107.
770 Costantini, F. et al., 2010. Deep-water *Corallium rubrum* (L., 1758) from the Mediterranean Sea:
771 preliminary genetic characterisation. Marine Ecology-an Evolutionary Perspective, 31(2): 261-
772 269.
773 Crerar, D.A., Barnes, H.L., 1974. Deposition of deep-sea manganese nodules. Geochimica et
774 Cosmochimica Acta, 38: 279-300.
775 Daumalin, X., Raveux, O., 2016. The Calanques: a dumping ground for high-pollution industries. In:
776 Daumalin, X., Laffont-Schwob, I. (Eds.), Pollution of Marseille's industrila Calanques. The
777 impact of the past on the present. REF.2C Editions, pp. 12-91.
778 Desenfant, F., Veron, A.J., Camoin, G.F., Nyberg, J., 2006. Reconstruction of pollutant lead invasion
779 into the tropical North Atlantic during the twentieth century. Coral Reefs, 25(3): 473-484.
780 Elbaz-Poulichet, F., Dezileau, L., Freydier, R., Cossa, D., Sabatier, P., 2011. A 3500-year record of Hg
781 and Pb contamination in a Mediterranean sedimentary archive (the Pierre Blanche Lagoon,
782 France). Environ Sci Technol, 45(20): 8642-7.
783 Epstein, S., Lowenstam, H.A., 1953. Temperature-shell-growth relations of recent interglacial
784 Pleistocene shoal-water biota from Bermuda. Journal of Geology, 61: 424-438.
785 Esslemont, G., 2000. Heavy metals in seawater, marine sediments and corals from the Townsville
786 section, Great Barrier Reef Marine Park, Queensland. Marine Chemistry, 71(3-4): 215-231.
787 Ferrand, J.L., Hamelin, B., Monaco, A., 1999. Isotopic tracing of anthropogenic Pb inventories and
788 sedimentary fluxes in the Gulf of Lions (NW Mediterranean sea). Continental Shelf Research,
789 19(1): 23-47.
790 Gagnon, J.E., Fryer, B.J., Samson, I.M., Williams-Jones, A.E., 2008. Quantitative analysis of silicate
791 certified reference materials by LA-ICPMS with and without an internal standard. Journal of
792 Analytical Atomic Spectrometry, 23(11): 1529.
793 Garrabou, J., Harmelin, J.G., 2002. A 20-year study on life-history traits of a harvested long-lived
794 temperate coral in the NW Mediterranean: insights into conservation and management
795 needs. Journal of Animal Ecology, 71(6): 966-978.
796 Gillikin, D.P. et al., 2005. Inter- and intra-annual variations of Pb/Ca ratios in clam shells (*Mercenaria*
797 *mercenaria*): a record of anthropogenic lead pollution? Mar Pollut Bull, 50(12): 1530-40.
798 Glasby, G.P., Schulz, H.D., 1999. E-H, pH diagrams for Mn, Fe, Co, Ni, Cu and As under seawater
799 conditions: Application of two new types of E-H, pH diagrams to the study of specific
800 problems in marine geochemistry. Aquatic Geochemistry, 5(3): 227-248.
801 Gosselin, M. et al., 2006. Trace metal concentrations in *Posidonia oceanica* of North Corsica
802 (northwestern Mediterranean Sea): use as a biological monitor? BMC Ecology: 1-19.
803 Hanna, R.G., Muir, G.L., 1990. Red-Sea Corals as Biomonitors of Trace-Metal Pollution. Environmental
804 Monitoring and Assessment, 14(2-3): 211-222.
805 Hasegawa, H., Iwasaki, N., Suzuki, A., Maki, T., Hayakawa, S., 2010. Distributions of Trace Elements in
806 Biogenic Carbonate Minerals of Precious Corals by X-ray Fluorescence Analysis. Bunseki
807 Kagaku, 59(6): 521-530.
808 Hong, S.M., Candelone, J.P., Patterson, C.C., Boutron, C.F., 1994. Greenland Ice Evidence of
809 Hemispheric Lead Pollution 2-Millennia Ago by Greek and Roman Civilizations. Science,
810 265(5180): 1841-1843.

811 Inoue, M. et al., 2006. Distribution and temporal changes of lead in the surface seawater in the
812 western Pacific and adjacent seas derived from coral skeletons. Environ Pollut, 144(3): 1045-
813 52.
814 Kaufman, A., Ghaleb, B., Wehmiller, J.F., HillaireMarcel, C., 1996. Uranium concentration and isotope
815 ratio profiles within *Mercenaria* shells: Geochronological implications. Geochimica et
816 Cosmochimica Acta, 60(19): 3735-3746.
817 Kelly, A.E., Reuer, M.K., Goodkin, N.F., Boyle, E.A., 2009. Lead concentrations and isotopes in corals
818 and water near Bermuda, 1780–2000. Earth and Planetary Science Letters, 283(1-4): 93-100.
819 Knittweis, L. et al., 2016. New depth record of the precious red coral *Corallium rubrum* for the
820 Mediterranean.
821 Lacaze-Duthiers, H., 1864. Histoire naturelle du corail J. B. Bailière et Fils, Paris.
822 Laffont-Schwob, I. et al., 2016. Diffuse and widespread present-day pollution. In: Daumalin, X.,
823 Laffont-Schwob, I. (Eds.), Pollution of Marseille's industrial Calanques. The impact of the past
824 on the present., pp. 205-249.
825 Lazareth, C.E. et al., 2000. Sclerosponges as a new potential recorder of environmental changes: Lead
826 in *Ceratoporella nicholsoni*. Geology, 28(6): 515-518.
827 Lee, J.M. et al., 2014. Coral-based history of lead and lead isotopes of the surface Indian Ocean since
828 the mid-20th century. Earth and Planetary Science Letters, 398: 37-47.
829 Marschal, C., Garrabou, J., Harmelin, J.G., Pichon, M., 2004. A new method for measuring growth and
830 age in the precious red coral *Corallium rubrum* (L.). Coral Reefs, 23(3): 423-432.
831 Martinez-Cortizas, A., Pontevedra-Pombal, X., Novoa Munoz, J.C., Garcia-Rodeja, E., 1997. Four
832 thousand years of atmospheric Pb, Cd and Zn deposition recorded by the ombrotrophic peat
833 bog of Penido Vello (Northwestern Spain). Water Air Soil Pollution, 100: 387-403.
834 Martinez Cortizas, A., Lopez-Merino, L., Bindler, R., Mighall, T., Kylander, M.E., 2016. Early
835 atmospheric metal pollution provides evidence for Chalcolithic/Bronze Age mining and
836 metallurgy in Southwestern Europe. Sci Total Environ, 545-546: 398-406.
837 McConchie, D., Harriott, V.J., 1992. The partitioning of metals between tissues and skeletal parts of
838 corals: application in pollution monitoring., 7th International Coral Reef Symposium.
839 University of Guam Marine Laboratory, Guam, Mangilao, pp. 97-103.
840 McConnell, J.R., Lamorey, G.W., Hutterli, M.A., 2002. A 250-year high-resolution record of Pb flux and
841 crustal enrichment in central Greenland. Geophysical Research Letters, 29(23): 45-1-45-4.
842 Medina-Elizalde, M., Gold-Bouchot, G., Ceja-Moreno, V., 2002. Lead contamination in the Mexican
843 Caribbean recorded by the coral *Montastraea annularis* (Ellis and Solander). Mar Pollut Bull,
844 44(5): 421-423.
845 Migon, C., Robin, T., Dufour, A., Gentili, B., 2008. Decrease of lead concentrations in the Western
846 Mediterranean atmosphere during the last 20 years. Atmospheric Environment, 42(4): 815-
847 821.
848 Mikac, N., Branicaa, M., Harrisonb, R.M., 2015. Total and organic lead distribution in water, sediment
849 and organisms from the Eastern Adriatic coast. Chemical Speciation & Bioavailability, 13(4):
850 121-128.
851 Miralles, J. et al., 2006. Atmospheric lead fallout over the last century recorded in Gulf of Lions
852 sediments (Mediterranean Sea). Mar Pollut Bull, 52(11): 1364-71.
853 Murozumi, M., Chow, T.J., Patterson, C.C., 1969. Chemical concentrations of pollutant lead aerosols,
854 terrestrial dusts and sea salts in Greenland and Antarctic snow strata. Geochimica et
855 Cosmochimica Acta, 33: 1247-1294.
856 Mutchler, S.R., Fedele, L., Bodnar, R.J., 2008. Analysis Management System (AMS) for reduction of
857 laser ablation ICPMS data. In: Sylvester, P. (Ed.), Laser-Ablation-ICPMS in the Earth Sciences:
858 Current Practices and Outstanding Issues. Mineralogical Association of Canada Short Course
859 Series. Mineralogical Association of Canada, Quebec, pp. 318-327.
860 Nicolas, E., Ruizpino, D., Buatmenard, P., Bethoux, J.P., 1994. Abrupt Decrease of Lead Concentration
861 in the Mediterranean-Sea - a Response to Antipollution Policy. Geophysical Research Letters,
862 21(19): 2119-2122.

863 Nozaki, Y., Thomson, J., Turekian, K.K., 1976. Distribution of ^{210}Pb and ^{210}Po in surface waters of
864 Pacific Ocean. Earth and Planetary Science Letters, 32(2): 304-312.
865 Nriagu, J.O., 1990. The rise and fall of leaded gasoline. Science of The Total Environment, 92: 13-28.
866 Nriagu, J.O., 1998. Tales told in lead (vol 281, pg 1622, 1998). Science, 282(5386): 51-51.
867 Pacyna, E.G. et al., 2007. Current and future emissions of selected heavy metals to the atmosphere
868 from anthropogenic sources in Europe. Atmospheric Environment, 41(38): 8557-8566.
869 Pacyna, J.M., Pacyna, P.E., 2000. Atmospheric emissions of anthropogenic lead in Europe:
870 improvements, updates, historical data and projections, Hagan, Norway.
871 Paraskevopoulou, V. et al., 2014. Trace metal variability, background levels and pollution status
872 assessment in line with the water framework and Marine Strategy Framework EU Directives
873 in the waters of a heavily impacted Mediterranean Gulf. Mar Pollut Bull, 87(1-2): 323-337.
874 Patterson, C.C., 1965. Contaminated and Natural Lead Environments of Man. Archives of
875 Environmental Health: An International Journal, 11(3): 344-360.
876 Perrin, J., 2014. Structure et squelettogenèse chez le genre *Corallium*, Aix-Marseille Université, 175
877 pp.
878 Perrin, J. et al., 2015. Block-by-block and layer-by-layer growth modes in coral skeletons. American
879 Mineralogist, 100(4): 681-695.
880 Rajola, G., 2012. The Sciacca mystery. Edizioni Scientifiche e Artistiche, 258 pp.
881 Rosenheim, B.E., Swart, P.K., Thorrold, S.R., 2005. Minor and trace elements in sclerosponge
882 *Ceratoporella nicholsoni*: Biogenic aragonite near the inorganic endmember?
883 Palaeogeography Palaeoclimatology Palaeoecology, 228(1-2): 109-129.
884 Serrano, O. et al., 2011. The Posidonia oceanica marine sedimentary record: A Holocene archive of
885 heavy metal pollution. Science of The Total Environment, 409(22): 4831-4840.
886 Settle, D.M., Patterson, C.C., 1980. Lead in Albacore - Guide to Lead Pollution in Americans. Science,
887 207(4436): 1167-1176.
888 Shannon, R.D., 1976. Revised Effective Ionic-Radii and Systematic Studies of Interatomic Distances in
889 Halides and Chalcogenides. Acta Crystallographica Section A, 32(Sep1): 751-767.
890 Shen, G.T., Boyle, E.A., 1987. Lead in corals - Reconstruction of historical industrial fluxes to the
891 surface ocean. Earth and Planetary Science Letters, 82(3-4): 289-304.
892 Shen, G.T., Boyle, E.A., 1988. Determination of Lead, Cadmium and Other Trace-Metals in Annually-
893 Banded Corals. Chemical Geology, 67(1-2): 47-62.
894 Shotyk, W., Le Roux, G., 2005. Biogeochemistry and cycling of lead. Biogeochemical Cycles of
895 Elements, 43: 239-275.
896 Shotyk, W. et al., 1998. History of atmospheric lead deposition since 12,370 ^{14}C yr BP from a peat
897 bog, Jura Mountains, Switzerland. Science, 281(5383): 1635-1640.
898 Sinclair, D.J. et al., 2011. Reproducibility of trace element profiles in a specimen of the deep-water
899 bamboo coral *Keratoisis sp*. Geochimica et Cosmochimica Acta, 75(18): 5101-5121.
900 Skeates, R., 1993. Mediterranean coral: its use and exchange in and around the alpine region during
901 the later Neolithic and copper age. Oxford Journal of Archaeology, 12: 281-292.
902 Swart, P.K., 2015. The geochemistry of carbonate diagenesis: The past, present and future.
903 Sedimentology, 62(5): 1233-1304.
904 Thomson, J. et al., 1986. The Behavior of Manganese in Atlantic Carbonate Sediments. Geochimica et
905 Cosmochimica Acta, 50(8): 1807-1818.
906 Tranchina, L., Micciche, S., Bartolotta, A., Brai, M., Mantegna, R.N., 2005. *Posidonia oceanica* as a
907 historical monitor device of lead concentration in marine environment. Environ Sci Technol,
908 39(9): 3006-3012.
909 Turicchia, E., Abbiati, M., Sweet, M., Ponti, M., 2018. Mass mortality hits gorgonian forests at
910 Montecristo Island. Diseases of Aquatic Organisms, 131(1): 79-85.
911 Ullmann, C.V., Korte, C., 2015. Diagenetic alteration in low-Mg calcite from macrofossils: a review.
912 Geological Quarterly, 59(1): 3-20.
913 Van Achterbergh, E., Ryan, C.G., Jackson, S.E., Griffin, W.L., 2001,, 2001. Data reduction software for
914 LA-ICP-MS. In: Sylvester, P.J. (Ed.), Laser Ablation –ICP-Mass Spectrometry in the Earth

Sciences: Principles and Applications. Mineralogical Association of Canada Short Course Series, Ottawa, Ontario, Canada, pp. 239-243.
Vielzeuf, D. et al., 2010. Multilevel modular mesocrystalline organization in red coral. American Mineralogist, 95(2-3): 242-248.
Vielzeuf, D. et al., 2018. Growth Kinetics and Distribution of Trace Elements in Precious Corals. Frontiers in Earth Science, 6.
Vielzeuf, D., Garrabou, J., Baronnet, A., Grauby, O., Marschal, C., 2008. Nano to macroscale biomineral architecture of red coral (*Corallium rubrum*). American Mineralogist, 93(11-12): 1799-1815.
Vielzeuf, D. et al., 2013. Distribution of sulphur and magnesium in the red coral. Chemical Geology, 355: 13-27.
von Storch, H. et al., 2003. Four decades of gasoline lead emissions and control policies in Europe: a retrospective assessment. Science of The Total Environment, 311(1-3): 151-176.
Weinbauer, M.G., Brandstätter, F., Velimirov, B., 2000. On the potential use of magnesium and strontium concentrations as ecological indicators in the calcite skeleton of the red coral (*Corallium rubrum*). Marine Biology, 137: 801-809.
Wertime, T.A., 1973. The beginning of Metallurgy: a new look. Science, 182: 875-887.
Wu, J.F., Boyle, E.A., 1997. Lead in the western North Atlantic Ocean: Completed response to leaded gasoline phaseout. Geochimica et Cosmochimica Acta, 61(15): 3279-3283.
Zibrowius, H., Monteiro Marques, V., Grasshoff, M., 1984. La répartition du *Corallium rubrum* dans l(Atlantique (*Cnidaria* : *Anthozoa* : *Gorgonaria*). Théthys, 1(2): 163-170.